Improved Wideband Precoding with Arbitrary Subcarrier Grouping in MIMO-OFDM Systems

Hang Long, Kyeong Jin Kim, Wei Xiang, Shanshan Shen, Kan Zheng, and Wenbo Wang

Precoding in the multiple-input multiple-output orthogonal frequency division multiplexing system is investigated. In conventional wideband precoding (WBP), only one precoder, obtained from the decomposition of the subcarrier independent channel matrix, is used for all subcarriers. With an investigation of the relationship between the subcarrier independent channel matrix and the temporal/frequency channels, an improved WBP scheme is proposed for practical scenarios in which a part of subcarriers are allocated to a user. The improved WBP scheme is a generalized scheme of which narrow-band precoding and conventional WBP schemes are special modes. Simulation results demonstrate that the improved WBP scheme almost achieves the optimum performance of a single precoder and outperforms the conventional WBP scheme in terms of the bit error ratio and ergodic capacity with slight complexity increase. The largest advantage of the improved WBP scheme on signal-to-noise ratio in simulation results is over 2.1 dB.

Keywords: MIMO, OFDM, wideband precoding.

Manuscript received Jan. 28, 2011; revised May 22, 2011; accepted June 23, 2011.

This research was supported by the National Basic Research Program of China (973 Program) under Grant 2012CB316005, the National Science Foundation for Post-doctoral Scientists of China under Grant 20110490329, and the Research Fund for the Doctoral Program of Higher Education 20090005120002.

Hang Long (phone: +86 10 62282245, hlong@buptnet.edu.cn), Shanshan Shen (shanchengfeiyan@gmail.com), Kan Zheng (zkan@bupt.edu.cn), and Wenbo Wang (wbwang@bupt.edu.cn) are with the Wireless Signal Processing and Network Lab, Key Laboratory of Universal Wireless Communication, Ministry of Education, Beijing University of Posts & Telecommunications, Beijing, China.

Kyeong Jin Kim (kyeong.j.kim@hotmail.com) is with the UWB Wireless Communications Research Center, Inha University, Incheon, Rep. of Korea.

Wei Xiang (Wei.Xiang@usq.edu.au) is with the Faculty of Engineering and Surveying, University of Southern Queensland, Toowoomba, QLD, Australia.

http://dx.doi.org/10.4218/etrij.12.0111.0050

I. Introduction

Recently, theoretical work has shown that in sufficiently rich scattering environments, multiple-input multiple-output (MIMO) systems hold the potential for tremendous spectral efficiency improvements [1]. On the other hand, the orthogonal frequency division multiplexing (OFDM) technique is widely used in high-data-rate wireless communication systems due to its high spectrum efficiency and tolerance of intersymbol-interference [2]-[4]. The MIMO-OFDM system has attracted significant worldwide research efforts.

Under the assumption that channel state information (CSI) is available at the transmitter, the performance of MIMO systems can be significantly improved with precoding techniques [5]-[8]. The well-known singular value decomposition (SVD)-based precoding technique [5], [6] can be used for channel diagonalization, whereas the QR decomposition (QRD)/ geometric mean decomposition (GMD)-based precoding schemes [7], [8] are used for channel trigonalization.

Conventional precoding schemes [5]-[8] are mostly proposed for narrow-band MIMO systems with flat-fading. These schemes are not suitable for MIMO-OFDM systems with frequency selective fading. It is neither possible nor necessary to compute one precoder for each subcarrier. The use of a single precoder for multiple continuous subcarriers is preferable.

Precoding with limited feedback has attracted significant attention in the past decade, for example, the vector quantization codebook-based scheme [9], the Grassmannian codebook-based scheme [10], [11], the interpolation based scheme [12], and the householder rotation-based scheme [13]. These schemes require sophisticated quantization to minimize information loss [14]. The complexity and feedback overhead of precoding in MIMO-OFDM systems can be further reduced.

A wideband precoding (WBP) scheme is presented in [14], [15], where only one precoder is used for all subcarriers in the MIMO-OFDM system. The precoder is obtained from the subcarrier independent channel matrix which is constructed through the temporal channel vectors. The CSI feedback overhead can be significantly reduced if the number of subcarriers is large.

In this paper, we point out that the WBP scheme in [14], [15] is suitable only when a single user is allocated with all subcarriers in the system. In practical OFDM systems, the number of available subcarriers is usually smaller than the discrete Fourier transform (DFT) size [3], [4]. Additionally, in the orthogonal frequency division multiple access (OFDMA) based cellular systems [3], all available subcarriers are allocated to multiple users according to their past and current channel gains [16]. The conventional WBP scheme in [14], [15] is not suitable for these scenarios, especially when the subcarriers allocated to a particular user are not continuous. Thus, improved WBP schemes for arbitrary subcarrier grouping are highly desirable.

The relationship between the subcarrier independent channel matrix and the temporal/frequency channel matrices is studied in this paper. Then, we propose an improved WBP scheme with arbitrary subcarrier grouping where a user is allocated with only part of all the subcarriers. The proposed scheme is shown to outperform the conventional WBP scheme, and performs similarly as the exhaustive optimum precoding scheme. Additionally, the improved WBP scheme includes the conventional one and narrow-band precoding schemes as its degraded modes. Simulation results validate the advantage of the proposed scheme. The advantage of the improved WBP scheme can be more significant if the group size is small or the subcarriers are not continuous.

The remainder of this paper is organized as follows. The system model is described in section II. The conventional WBP scheme is reviewed in section III and the improved WBP scheme is presented in section IV. Simulation results are given in section V. Finally, section VI concludes this paper.

Notation. $\mathbf{A}^{\mathrm{T}}$, $\mathbf{A}^{\mathrm{H}}$, and $\mathbf{A}^{-1}$ denote the transpose, conjugate-transpose, and pseudoinverse of matrix $\mathbf{A}$, respectively. $\mathbf{I}_n$ and $\mathbf{0}_{m,n}$ denote the $n\times n$ identity matrix and the $m\times n$ all-zero matrix, respectively. Mathematical expectation is denoted by $E(\cdot)$, and $\otimes$ denotes the Kronecker product of two matrices. The vector space of all $m\times n$ complex matrices is denoted by $\mathbb{C}^{m\times n}$. The largest integral smaller than x is denoted by $\lfloor x \rfloor$.

II. System Model

We consider the MIMO-OFDM system with a DFT size of

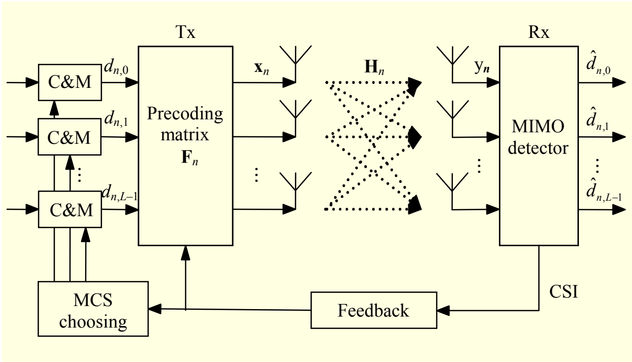

Fig. 1. Illustration of MIMO system over n-th subcarrier.

N and L input spatial streams. N_{T} and N_{R} antennas are equipped at the transmitter and receiver, respectively. $N_{\mathrm{T}} \geq L, N_{\mathrm{R}} \geq L$, and the maximum path delay is assumed to be shorter than the length of the cyclic prefix (CP).

The equivalent MIMO system over the n-th subcarrier can be written as

$$\mathbf{y}_n = \mathbf{H}_n \mathbf{x}_n + \mathbf{z}_n, \quad n \in \{0,1,\cdots,N-1\}, \tag{1}$$

where $\mathbf{x}_n \in \mathbb{C}^{N_{\mathrm{T}}\times 1}$ and $\mathbf{y}_n \in \mathbb{C}^{N_{\mathrm{R}}\times 1}$ are the transmitted and received signal vectors, respectively; $\mathbf{z}_n$ is the additive white Gaussian noise at the receiver, $\mathbf{z}_n \sim \mathcal{CN}(\mathbf{0}_{N_{\mathrm{R}},1}, \sigma^2 \mathbf{I}_{N_{\mathrm{R}}})$; and $\mathbf{H}_n \in \mathbb{C}^{N_{\mathrm{R}}\times N_{\mathrm{T}}}$ is the frequency MIMO channel matrix over the n-th subcarrier.

The equivalent MIMO system is also illustrated in Fig. 1, where $d_{n,i}$ is the modulated symbol of the i-th spatial data stream over the n-th subcarrier, $i \in \{0,1,\cdots,L-1\}$, that is, $\mathbf{d}_n = [d_{n,1}, d_{n,2}, \cdots, d_{n,L}]^{\mathrm{T}}$ is the data vector before precoding. It is assumed that

$$E(\mathbf{d}_n \mathbf{d}_{n'}^H) = \begin{cases} \frac{1}{L}\mathbf{I}_L, & n = n', \\ \mathbf{0}_{L,L}, & n \neq n'. \end{cases} \tag{2}$$

$\mathbf{F}_n$ is the precoder over the n-th subcarrier, and $\mathbf{x}_n = \mathbf{F}_n \mathbf{d}_n$.

As described in [14], [15], $\mathbf{H}_n$ in (1) can also be denoted by the temporal channels. $h_l^{p,q}$ is the temporal channel of the l-th tap between the p-th transmit antenna and the q-th receive antenna, $l \in \{0,1,\cdots,N_f-1\}$, $p \in \{1,2,\cdots,N_{\mathrm{T}}\}$, and $q \in \{1,2,\cdots,N_{\mathrm{R}}\}$. N_f denotes the channel order determined by the following equation

$$N_f = \left\lfloor \frac{\tau_{\max}}{\Delta t} \right\rfloor + 1, \tag{3}$$

where $\tau_{\max}$ is the maximum path delay, and Δt is the temporal sampling interval. The temporal channel vector between the p-th transmit antenna and the q-th receive antenna can be written as

$$\mathbf{h}^{p,q} = [h_0^{p,q}, h_1^{p,q}, \cdots, h_{N_f-1}^{p,q}]^{\mathrm{T}}. \quad (4)$$

Using (4), $\mathbf{H}_n$ can be written in terms of $\mathbf{h}^{p,q}$ as in [14], [15]

$$\mathbf{H}_n = \begin{bmatrix} \mathbf{w}_n^{\mathrm{T}}\mathbf{h}^{1,1} & \cdots & \mathbf{w}_n^{\mathrm{T}}\mathbf{h}^{N_{\mathrm{T}},1} \\ \vdots & \ddots & \vdots \\ \mathbf{w}_n^{\mathrm{T}}\mathbf{h}^{1,N_{\mathrm{R}}} & \cdots & \mathbf{w}_n^{\mathrm{T}}\mathbf{h}^{N_{\mathrm{T}},N_{\mathrm{R}}} \end{bmatrix}, \quad (5)$$

where

$$\mathbf{w}_n = [1, \mathrm{e}^{-j\cdot 2\pi n/N}, \mathrm{e}^{-j\cdot 2\pi n\cdot 2/N}, \cdots, \mathrm{e}^{-j\cdot 2\pi n\cdot (N_f-1)/N}]^{\mathrm{T}}. \quad (6)$$

III. Wideband Precoding

In the conventional narrow-band precoding scheme, if CSI is known at the transmitter, the optimum precoder over the n-th subcarrier can be achieved with the SVD of $\mathbf{H}_n$ [10], [11], [14]

$$\mathbf{H}_n = \mathbf{U}_n \mathbf{\Sigma}_n \mathbf{V}_n^{\mathrm{H}}, \quad (7)$$

$$\mathbf{F}_n = \mathbf{V}_n [\mathbf{I}_L, \mathbf{0}_{L,N_{\mathrm{T}}-L}]^{\mathrm{T}}. \quad (8)$$

A WBP scheme is presented in [14], [15], where only one precoder is used for all subcarriers. In this way, the CSI feedback overhead can be significantly reduced.

Equation (5) can be rewritten as

$$\mathbf{H}_n = \left(\mathbf{I}_{N_{\mathrm{R}}} \otimes \mathbf{w}_n^{\mathrm{T}}\right)\mathbf{H}, \quad (9)$$

where

$$\mathbf{H} = \begin{bmatrix} \mathbf{h}^{1,1} & \cdots & \mathbf{h}^{N_{\mathrm{T}},1} \\ \vdots & \ddots & \vdots \\ \mathbf{h}^{1,N_{\mathrm{R}}} & \cdots & \mathbf{h}^{N_{\mathrm{T}},N_{\mathrm{R}}} \end{bmatrix} \quad (10)$$

is the subcarrier independent channel matrix. The SVD of $\mathbf{H}$ is calculated at the receiver as [14], [15]

$$\mathbf{H} = \mathbf{U}\mathbf{\Sigma}\mathbf{V}^{\mathrm{H}}. \quad (11)$$

The first L-th singular vectors are used as the precoder, that is,

$$\mathbf{F}_n = \mathbf{F} = \mathbf{V}[\mathbf{I}_L, \mathbf{0}_{L,N_{\mathrm{T}}-L}]^{\mathrm{T}}, \quad n \in \{0, 1, \cdots, N-1\}. \quad (12)$$

In (12), $\mathbf{V}$ can also be obtained with the eigenvalue decomposition of $\mathbf{H}^{\mathrm{H}}\mathbf{H}$. The linear zero-forcing (ZF) equalizer is assumed to be employed in this study for simplicity.

We assume that all subcarriers are employed ($n \in \{0, 1, \cdots, N-1\}$). As mentioned before, this assumption is not valid for practical OFDMA systems. To overcome these difficulties, we propose an improved WBP scheme with arbitrary subcarrier grouping in the following section.

IV. Wideband Precoding with Arbitrary Subcarrier Grouping

An alternative explanation of the WBP scheme in [14], [15] is given in this section. Firstly, we investigate the relationship between the subcarrier independent channel matrix $\mathbf{H}$ and the temporal/frequency MIMO channel matrices. The temporal MIMO channel matrix of the i-th tap is constructed by $\{h_i^{p,q}\}$ as follows:

$$\mathbf{H}_i^{(\mathrm{t})} = \begin{bmatrix} h_i^{1,1} & \cdots & h_i^{N_{\mathrm{T}},1} \\ \vdots & \ddots & \vdots \\ h_i^{1,N_{\mathrm{R}}} & \cdots & h_i^{N_{\mathrm{T}},N_{\mathrm{R}}} \end{bmatrix}, \quad i \in \{0, 1, \cdots, N_f - 1\}. \quad (13)$$

The relationship between $\mathbf{H}$ and the temporal MIMO channel matrices $\{\mathbf{H}_i^{(\mathrm{t})}\}$ can be summarized as

$$\mathbf{H}^{\mathrm{H}}\mathbf{H} = \sum_{i=0}^{N_f-1} [\mathbf{H}_i^{(\mathrm{t})}]^{\mathrm{H}} \mathbf{H}_i^{(\mathrm{t})}. \quad (14)$$

That is, the covariance matrix of the subcarrier independent channel is the sum of the covariance matrices of the temporal MIMO channel matrices. The proof of (14) is straightforward, and thus we omit its details for brevity.

Proposition 1. The relationship between $\mathbf{H}$ and the frequency MIMO channel matrices $\{\mathbf{H}_n\}$ is given by

$$\mathbf{H}^{\mathrm{H}}\mathbf{H} = \frac{1}{N}\sum_{n=0}^{N-1} \mathbf{H}_n^{\mathrm{H}}\mathbf{H}_n. \quad (15)$$

That is, the covariance matrix of the subcarrier independent channel is the average of the covariance matrices of the frequency MIMO channel matrices.

Proof: According to (9), we have

$$\begin{aligned} \mathbf{H}_n^{\mathrm{H}}\mathbf{H}_n &= \mathbf{H}^{\mathrm{H}}\left(\mathbf{I}_{N_{\mathrm{R}}} \otimes \mathbf{w}_n^{\mathrm{T}}\right)^{\mathrm{H}}\left(\mathbf{I}_{N_{\mathrm{R}}} \otimes \mathbf{w}_n^{\mathrm{T}}\right)\mathbf{H} \\ &= \mathbf{H}^{\mathrm{H}}\left[\mathbf{I}_{N_{\mathrm{R}}} \otimes \left(\mathbf{w}_n^{*}\mathbf{w}_n^{\mathrm{T}}\right)\right]\mathbf{H}. \end{aligned} \quad (16)$$

The elements in matrix $\mathbf{w}_n^{*}\mathbf{w}_n^{\mathrm{T}}$ have the same modulus but different angles as

$$\mathbf{w}_n^{*}\mathbf{w}_n^{\mathrm{T}} = \mathrm{e}^{j2\pi\mathbf{\Theta}_n/N}, \quad (17)$$

and

$$\mathbf{\Theta}_n = \begin{bmatrix} 0 & -n & \cdots & -(N_f-1)n \\ n & 0 & \cdots & -(N_f-2)n \\ \vdots & \ddots & \ddots & \vdots \\ (N_f-1)n & (N_f-2)n & \cdots & 0 \end{bmatrix} \quad (18)$$

is the phase offset matrix satisfying $\mathbf{\Theta}_n + \mathbf{\Theta}_n^{\mathrm{T}} = \mathbf{0}_{N_f,N_f}$. Due to the property of

$$\sum_{n=0}^{N-1} \mathrm{e}^{j2\pi nk/N} = \begin{cases} 0, & k \in \{-N+1, \cdots, -1, 1, 2, \cdots, N-1\}, \\ N, & k = 0, \end{cases} \quad (19)$$

we have

$$\frac{1}{N}\sum_{n=0}^{N-1}\left(\mathbf{w}_n^* \mathbf{w}_n^{\mathrm{T}}\right) = \mathbf{I}_{N_f}. \quad (20)$$

According to (16) and (20), (15) is proved. □

As shown in proposition 1, the precoder in (12) is obtained from the average covariance matrix of the frequency MIMO channels over all the N subcarriers. Hence, it can be considered as an average choice for precoding through N subcarriers. However, the number of available subcarriers is usually smaller than the DFT size N in practical systems. For example, in the third generation partnership project (3GPP) long term evolution (LTE) system [2], [3] with a bandwidth of 10 MHz, 600 subcarriers are used while the DFT size is 1,024. Besides, in OFDMA systems, all available subcarriers are allocated to multiple users. Conventional WBP schemes can be further improved if a user is allocated with a set of subcarriers. For special scenarios where only one subcarrier is allocated to the user, for example, the n-th subcarrier, $\mathbf{H}$ is so different from $\mathbf{H}_n$ that the conventional WBP scheme is much worse than the optimum precoder given in (8).

Proposition 1 motivates us to propose an improved WBP scheme, where the precoder is calculated by the averaged covariance matrix of the channel matrices over the subcarriers that are allocated to the user. It is assumed that the user is allocated with a subcarrier group: $n \in \mathcal{S} \subset \{0, 1, \cdots, N-1\}$. We define the average covariance matrix as

$$\mathbf{R}_{\mathcal{S}} = \frac{1}{|\mathcal{S}|}\mathbf{H}^{\mathrm{H}}\left[\mathbf{I}_{N_{\mathrm{R}}} \otimes \sum_{n\in\mathcal{S}}\left(\mathbf{w}_n^* \mathbf{w}_n^{\mathrm{T}}\right)\right]\mathbf{H}, \quad (21)$$

where $|\mathcal{S}|$ is the number of subcarriers in $\mathcal{S}$. The eigenvalue decomposition of $\mathbf{R}_{\mathcal{S}}$ is carried out at the receiver as

$$\mathbf{R}_{\mathcal{S}} = \mathbf{E}\boldsymbol{\Pi}\mathbf{E}^{\mathrm{H}}, \quad (22)$$

where $\mathbf{E}$ is constructed with the eigenvectors of $\mathbf{R}_{\mathcal{S}}$, and $\boldsymbol{\Pi}$ is a diagonal matrix with the descendingly sorted eigenvalues of $\mathbf{R}_{\mathcal{S}}$. The precoder for $\mathcal{S}$ is constructed of the first L eigenvectors of $\mathbf{R}_{\mathcal{S}}$:

$$\mathbf{F}_n = \mathbf{E}\left[\mathbf{I}_L, \mathbf{0}_{L,N_{\mathrm{T}}-L}\right]^{\mathrm{T}}. \quad (23)$$

Similar to the conventional WBP scheme in (10) to (12), only one precoder is required for the improved scheme. Thus, the CSI feedback overhead of the improved WBP scheme is the same as the conventional one in [14], [15]. Note that if only one subcarrier is allocated to the user, for example, $\mathcal{S} = \{n\}$, the precoder in (23) degrades to the conventional narrow-band precoder in (8). Hence, the improved WBP scheme includes the conventional narrow-band precoding scheme and the conventional WBP scheme in [14], [15] ($\mathcal{S} = \{0, 1, \cdots, N-1\}$) as special degraded modes. Similarly, QRD/GMD can also be utilized in the improved WBP scheme.

If a small number of subcarriers are allocated to the user, the conventional WBP scheme cannot utilize the subcarrier group information, whereas the improved one is able to make use of the information for the precoding design as shown in (21). Intuitively, the improved WBP scheme outperforms the conventional one if the size of subcarrier group is small and $\mathbf{H}^{\mathrm{H}}\mathbf{H}$ is quite different from $\mathbf{R}_{\mathcal{S}}$. These properties will be verified by the simulations in section V.

As shown in (21), subcarrier group information is required both at both the transmitter and the receiver. Thus, additional signaling overhead between the transmitter and receiver is inevitable in OFDMA systems with the use of subcarrier scheduling even if the improved WBP scheme is not in use. For example, in the 3GPP LTE downlink system, subcarrier allocation information belonging to each user is transmitted through the so-called physical downlink control channel which occupies the first three OFDM symbols of each subframe [3]. However, the proposed improved WBP scheme does not require additional signaling overhead in OFDMA systems.

Compared (21) to (23) with (10) to (12), the proposed WBP scheme slightly increases the computational complexity of the receiver. Once the subcarriers are allocated to the user, the group relative matrix can be calculated as

$$\sum_{n\in\mathcal{S}}\left(\mathbf{w}_n^* \mathbf{w}_n^{T}\right). \quad (24)$$

Then, it can be used until the subcarrier allocation is changed. The decompositions in (22) and (11) require the same operations. The computation of (24) entails around about $|\mathcal{S}|N_f^2$ complex additions, and that of (21) requires two additional matrix multiplications at the receiver for each subframe, namely, less than $N_{\mathrm{T}}N_f(N_fN_{\mathrm{R}} + N_{\mathrm{T}})$ complex multiplications. Compared with the complexity of the SVD and other matrix operations, the additional computational complexity with the improved WBP scheme is nearly negligible.

V. Simulation Results

Our simulation parameters for performance evaluation are listed in Table 1. The ergodic capacity and bit error rate (BER) are adopted as the performance metrics. The system ergodic capacity is defined as [17], [18]

Table 1. System parameters.

Sampling frequency ($1/\Delta t$)	960 kHz
DFT size (N)	64
Available subcarriers	64
OFDM symbol duration	Data: 66.67 µs CP: 4.56 µs
Length of subframe	1 ms (14 OFDM symbols)
Channel estimation	ideal
Synchronization	ideal
Antenna configuration ($N_T \times N_R$)	2×2, 4×4
Number of data streams (L)	1, 2, 3
Channel model	Pedestrian B in [19]
N_f	4
MS speed	3 km/h
Modulation	Binary phase-shift keying (BPSK)
MIMO equalization	ZF

$$C = \frac{1}{|\mathcal{S}|}\sum_{n\in\mathcal{S}}\sum_{i=0}^{L-1} E\left[\log_2(1+\gamma_{n,i})\right], \qquad (25)$$

where $\gamma_{n,i}$ is the *post*-SNR of the *i*-th data stream over the *n*-th subcarrier after ZF equalization.

Some reference schemes are also evaluated for purpose of performance comparison. The precoder with exhaustive search is used as the performance upper bound. A vast number of unit vectors/unitary matrices are randomly generated and the one with the optimum capacity/BER performance is selected according to

$$\mathbf{F}_n = \arg\max_{\mathbf{F}} C(\mathbf{F}) \qquad (26)$$

and

$$\mathbf{F}_n = \arg\min_{\mathbf{F}} \mathrm{BER}(\mathbf{F}). \qquad (27)$$

The precoder with exhaustive search is denoted by "ESP" in the sequel. Note that the results of (26) and (27) are different.

Three subcarrier groups are considered in simulations: i) $\mathcal{S}_1 = \{0,1,\cdots,31\}$; ii) $\mathcal{S}_2 = \{0,1,\cdots,15,32,33,\cdots,47\}$; and iii) $\mathcal{S}_3 = \{0,1,\cdots,15\}$. It is intuitive that the conventional WBP scheme performs poorly with $\mathcal{S}_3$ since the number of allocated subcarriers is small and the matrix in (24) is far from a scaled identity matrix. The improved WBP scheme outperforms its conventional counterpart for any subcarrier grouping. The simulation results will validate the analytical conclusion drawn in the preceding section.

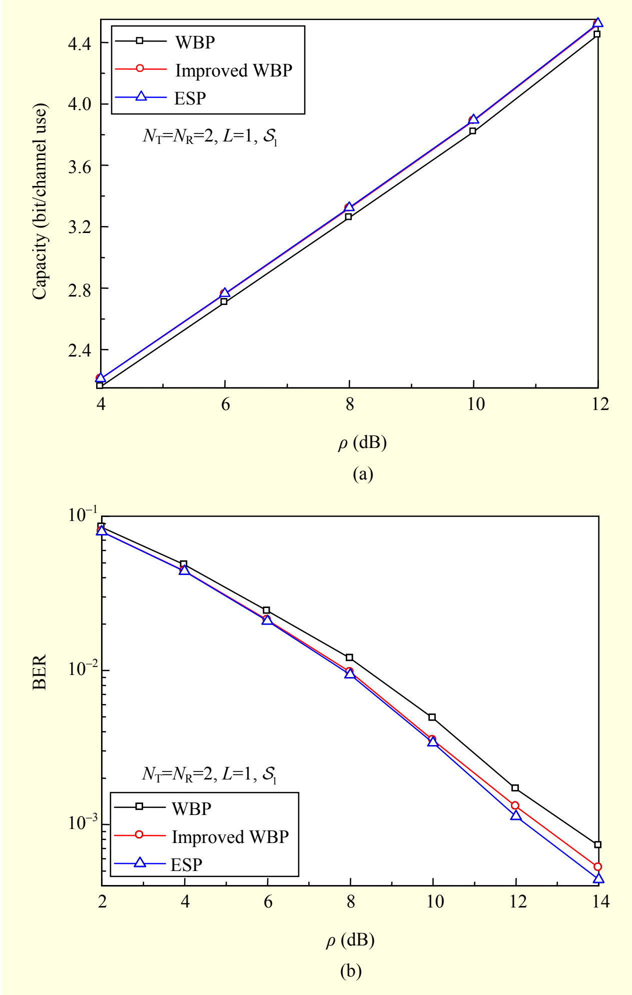

Fig. 2. (a) Capacity performance and (b) BER performance with N_T=N_R=2, L=1, and $\mathcal{S}_1$.

The capacity and BER performance comparison with N_T=N_R=2 and $\mathcal{S}_1$ is shown in Fig. 2. The precoder is a 2×1 vector, which makes exhaustive search possible. 1,000 vectors are randomly generated at each subframe to find the optimum precoder defined in (26) or (27). With the increase of N_T, exhaustive search grows in prohibitive complexity, so that the results of ESP cannot be shown in Figs. 3 to 5.

Similar ergodic capacities for the three precoding schemes can be observed in Fig. 2. Since only half of the subcarriers are allocated to the user, the improved WBP scheme performs closely to the optimum ESP scheme and outperforms the conventional WBP scheme by 0.2 dB as shown in Fig. 2(a) where the curves with the circle and upper triangle symbols are almost overlapped. The differences in the BER among the three schemes are noticeable in Fig. 2(b). The improved WBP scheme outperforms the conventional one by about 0.7 dB at BER=10^{-3}.

More antennas at the transmitter and receiver are considered

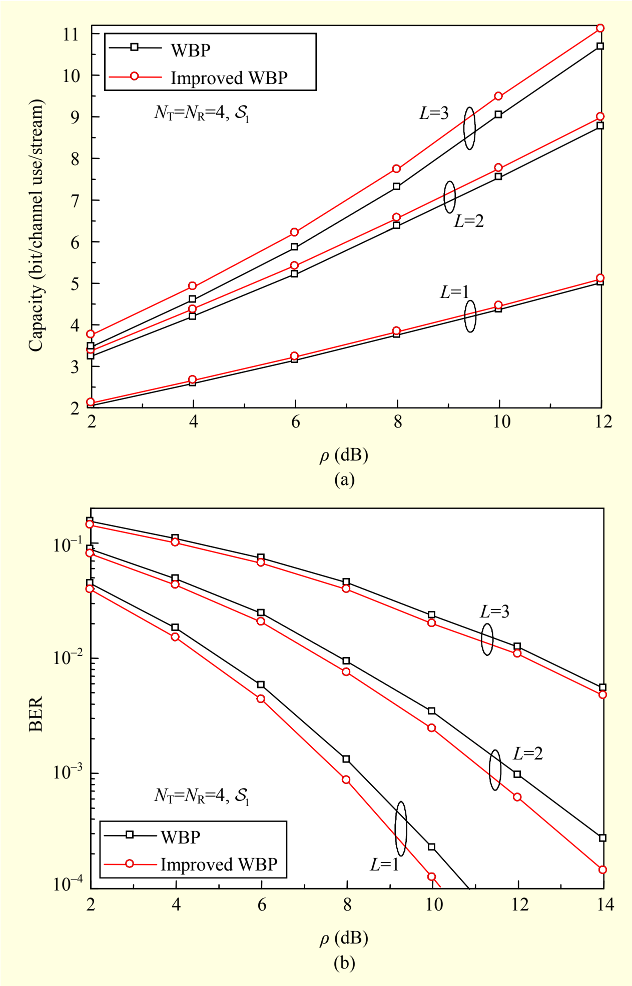

Fig. 3. (a) Capacity performance and (b) BER performance with N_T=N_R=4, L=1, 2, 3, and $\mathcal{S}_1$.

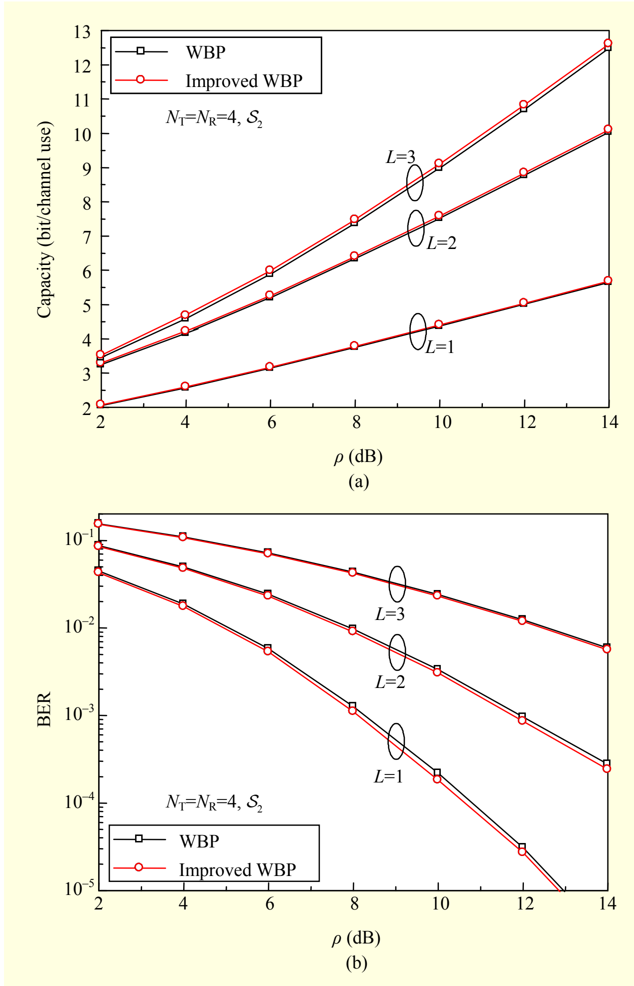

Fig. 4. (a) Capacity performance and (b) BER performance with N_T=N_R=4, L=1, 2, 3, and $\mathcal{S}_2$.

in Figs. 3 to 5 with the three subcarrier groups. The improved WBP scheme achieves a better performance than the conventional one for any subcarrier grouping and number of data streams. Since only half of the subcarriers are allocated to the user with $\mathcal{S}_1$, and the frequency independent channel matrix in (10) cannot represent the frequency channels of the first $N/2$ subcarriers. In Fig. 3(a), the improvement between the two schemes becomes noticeable when L is large. The observation of Fig. 3(b) is contrary since the BER performance with large L is worse than that with a small number of data streams. The improved WBP scheme outperforms the conventional one by about 0.5 dB in the average SNR at C=8.0 bits/channel use and L=3. This is observed in Fig. 3(a). The largest improvement in the SNR in Fig. 3(b) is about 0.6 dB for BER=10^{-4} with L=1.

Similar observations can be obtained from Figs. 4 and 5. With $\mathcal{S}_2$, the subcarriers are not continuous and the group relative matrix in (24) is close to a scaled identity matrix, so that the frequency independent channel $\mathbf{H}$ can be approximately used to compute the precoder. The conventional and improved WBP schemes perform similarly as shown in Fig. 4. The advantage of the improved WBP scheme is more evident for $\mathcal{S}_3$ as shown in Fig. 5, since the size of $\mathcal{S}_3$ is smaller than those of $\mathcal{S}_1$ and $\mathcal{S}_2$. The largest distance between the two curves shown in Fig. 5(b) is about 2.1 dB.

According to the simulation results, the proposed WBP scheme achieves near optimum capacity and BER performance. Additionally, it outperforms the conventional WBP scheme for arbitrary subcarrier grouping. The performance difference becomes noticeable when a small number of continuous subcarriers are allocated to the user.

VI. Conclusion

WBP with one precoder for all subcarriers allocated to users in the MIMO-OFDM system is investigated in this paper. The conventional WBP scheme is shown to be feasible only when all subcarriers are allocated to a particular user. The relationship

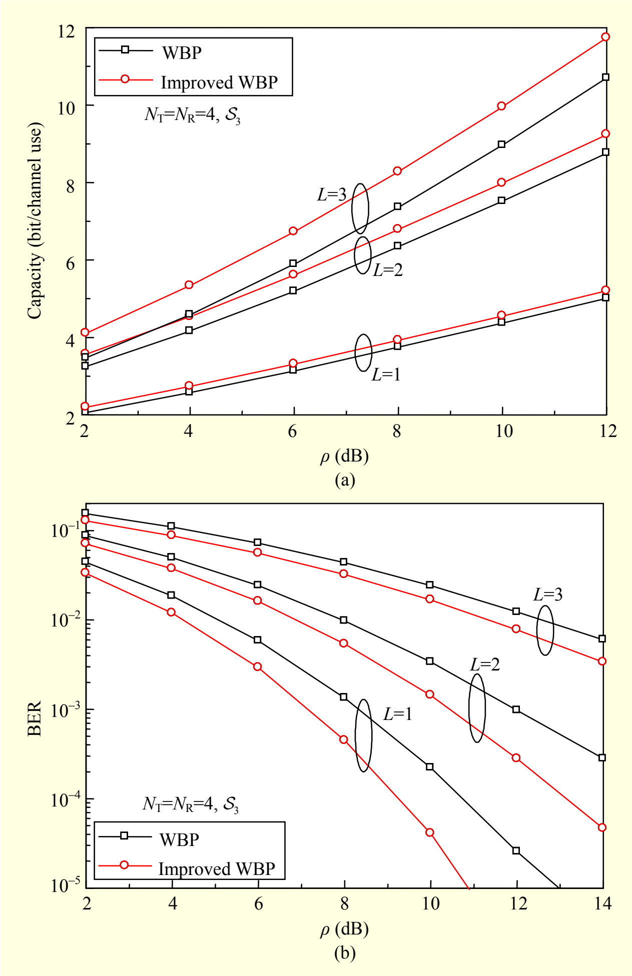

Fig. 5. (a) Capacity performance and (b) BER performance with N_T=N_R=4, L=1, 2, 3, and $\mathcal{S}_3$.

between the subcarrier independent channel matrix and the temporal/frequency channel matrices is derived. Then, an improved WBP scheme with arbitrary subcarrier grouping is proposed, which includes the conventional WBP and narrow-band precoding schemes as special degraded modes. Simulation results verify that the improved WBP scheme achieves near optimum capacity and BER performance and outperforms the conventional WBP scheme, especially when the allocated subcarriers are located within a small bandwidth.

References

[1] G.J. Foschini and M.J. Gans, "On Limits of Wireless Communications in a Fading Environment When Using Multiple Antennas," *Wireless Personal Commun.*, vol. 6, no. 3, Mar. 1998, pp. 311-335.

[2] 3GPP TR 36.814 v9.0.0, "Further Advancements for E-UTRA Physical Layer Aspects (Release 9)," Mar. 2010. Available: http://www.3gpp.org/ftp

[3] 3GPP TS 36.211 v8.8.0, "Physical Channels and Modulation," Sept. 2009. Available: http://www.3gpp.org/ftp

[4] IEEE P802.11n/D1.04, "Wireless LAN Medium Access Control (MAC) and Physical Layer (PHY) Specifications: Enhancements for Higher Throughput," Sept. 2006.

[5] G.G. Raleigh and J.M. Cioffi, "Spatio-Temporal Coding for Wireless Communication," *IEEE Trans. Commun.*, vol. 46, no. 3, Mar. 1998, pp. 357-366.

[6] A. Scaglione, S. Barbarossa, and G.B. Giannakis, "Filterbank Transceivers Optimizing Information Rate in Block Transmissions over Dispersive Channels," *IEEE Trans. Inf. Theory*, vol. 45, no. 3, Apr. 1999, pp. 1019-1032.

[7] J. Zhang and K.J. Kim, "Near-Capacity MIMO Multiuser Precoding with QRD-M Algorithm," *Proc. Asilomar Conf. Signals, Syst., Comput.*, Pacific Grove, CA, USA, 2005, pp. 1498-2002.

[8] Y. Jiang, J. Li, and W. Hager, "Joint Transceiver Design for MIMO Communications Using Geometric Mean Decomposition," *IEEE Trans. Signal Process.*, vol. 53, no. 10, Oct. 2005, pp. 3791-3803.

[9] J.C. Roh and B.D. Rao, "Transmit Beamforming in Multiple-Antenna Systems with Finite Rate Feedback: A VQ-Based Approach," *IEEE Trans. Inf. Theory*, vol. 52, no. 3, Mar. 2006, pp. 1101-1112.

[10] D.J. Love and R.W. Heath Jr., "Limited Feedback Precoding for Spatial Multiplexing Systems," *Proc. IEEE Globecom*, vol. 4, San Francisco, CA, USA, Dec. 2003, pp. 1857-1861.

[11] D.J. Love, R.W. Heath Jr., and T. Strohmer, "Grassmannian Beamforming for Multiple-Input Multiple-Output Wireless Systems," *IEEE Trans. Inf. Theory*, vol. 49, no. 10, Oct. 2003, pp. 2735-2747.

[12] J. Choi and R.W. Heath Jr., "Interpolation Based Transmit Beamforming for MIMO-OFDM with Limited Feedback," *IEEE Trans. Signal Process.*, vol. 53, no. 11, Nov. 2005, pp. 4125-4135.

[13] Q. Li and X. Lin, "Compact Feedback for MIMO-OFDM Systems over Frequency Selective Channels," *Proc. IEEE VTC Spring*, Stockholm, Sweden, May 2005, pp. 187-191.

[14] K.J. Kim, M.O. Pun, and R.A. Iltis, "QRD-Based Precoded MIMO-OFDM Systems with Reduced Feedback," *IEEE Trans. Comm.*, vol. 58, no. 2, Feb. 2010, pp. 394-398.

[15] K.J. Kim, M.O. Pun, and R.A. Iltis, "QRD-Based Precoded MIMO-OFDM Systems with Reduced Feedback," *Proc. IEEE ICC*, Beijing, China, May 2008, pp. 708-712.

[16] H. Kim et al., "A Proportional Fair Scheduling for Multicarrier Transmission Systems," *Proc. IEEE VTC2004-Fall*, LA, CA, USA, 2004, pp. 409-413.

[17] H. Bolcskei, D. Gesbert, and A.J. Paulraj, "On the Capacity of OFDM-Based Spatial Multiplexing Systems," *IEEE Trans. Comm.*, vol. 50, no. 2, Feb. 2002, pp. 225-234.

[18] S. Gault, W. Hachem, and P. Ciblat, "Performance Analysis of an

OFDMA Transmission System in a Multicell Environment," *IEEE Trans. Comm.*, vol. 55, no. 4, Apr. 2007, pp. 740-751.
[19] 3GPP TR 25.996 v6.1.0, "Spatial Channel Model for Multiple Input Multiple Output (MIMO) Simulations (Release 6)," Sept. 2003. Available: http://www.3gpp.org/ftp

Hang Long received the BS and PhD from Beijing University of Posts and Telecommunications (BUPT), Beijing, China, in 2005 and 2010, respectively. Since 2010, he has been with BUPT as a postdoctoral researcher. His current research interests are in the field of signal processing for wireless communications with emphasis on MIMO and cooperative communications.

Kyeong Jin Kim received the MS from the Korea Advanced Institute of Science and Technology (KAIST) in 1991, and the PhD in electrical and computer engineering from the University of California, Santa Barbara, in 2000. During 1991 to 1995, he was a research engineer at the Video Research Center of Daewoo Electronics Ltd., Rep. of Korea. In 1997, he joined the Data Transmission and Networking Laboratory at the University of California, Santa Barbara, USA. After receiving his degrees, he joined the Nokia Research Center in Dallas as a senior research engineer. From 2005 to 2009, he worked with the Nokia Corporation in Dallas as a L1 specialist. His research has focused on the transceiver design, resource management, and scheduling in the wireless communication systems. He is currently working at Inha University, Rep. of Korea.

Wei Xiang received the BEng and MEng, both in electronic engineering, from the University of Electronic Science and Technology of China, Chengdu, China, in 1997 and 2000, respectively, and the PhD in telecommunications engineering from the University of South Australia, Adelaide, Australia, in 2004. Since 2004, he has been with the Faculty of Engineering and Surveying, University of Southern Queensland, Toowoomba, Australia, where he was first an associate lecturer in computer systems engineering from 2004 to 2006, then a lecturer from 2007 to 2008, and currently holds a faculty post of senior lecturer. In 2008, he was a visiting scholar at the School of Electrical and Electronic Engineering, Nanyang Technological University, Singapore. During 2010 and 2011, he was a visiting scholar at the University of Mississippi, Oxford, MS, USA. He was awarded a prestigious Queensland International Fellowship in 2010. His research interests are in the broad area of communications and information theory, particularly coding and signal processing for multimedia communications systems.

Shanshan Shen received the BS from Beijing University of Posts and Telecommunications (BUPT), Beijing, China, in 2009. Since 2009, she has been pursuing her MS at BUPT. Her current research interests are in the field of MIMO and cooperative systems.

Kan Zheng received the BS, MS, and PhD from Beijing University of Posts and Telecommunications (BUPT), Beijing, China, in 1996, 2000, and 2005, respectively. Since 2005, he has been with the Wireless Signal Processing and Network Lab, BUPT. Since 2008, he has been working at the School of Information and Telecommunication Engineering (SITE), BUPT, as an associate professor. His current research interests are in the field of signal processing for digital communications with emphasis on space-time coding and cooperative communications.

Wenbo Wang received the BS, MS, and PhD from Beijing University of Posts and Telecommunications (BUPT), Beijing, China, in 1986, 1989, and 1992, respectively. He is currently a professor and the Dean of the Graduate School, BUPT. His research interests include signal processing, mobile communications, and wireless ad hoc networks.